Fermi National Accelerator Laboratory

FERMILAB-Pub-77/107-EXP
7100.288

(Submitted to Phys. Rev. Lett.)

STUDY OF THE HIGH MASS DIMUON CONTINUUM IN 400 GeV PROTON-NUCLEUS COLLISIONS

D. M. Kaplan, R. J. Fisk, A. S. Ito, and H. Jöstlein
State University of New York at Stony Brook
Stony Brook, Long Island, New York 11794

and

J. A. Appel, B. C. Brown, C. N. Brown, W. R. Innes,
R. D. Kephart, K. Ueno, and T. Yamanouchi
Fermi National Accelerator Laboratory
Batavia, Illinois 60510

and

S. W. Herb, D. C. Hom, L. M. Lederman,
J. C. Sens, H. D. Snyder, and J. K. Yoh
Columbia University
New York, New York 10027

December 1977

Operated by Universities Research Association Inc. under contract with the Energy Research and Development Administration

STUDY OF THE HIGH MASS DIMUON CONTINUUM IN 400 GEV PROTON-NUCLEUS COLLISIONS

D. M. Kaplan, R. J. Fisk, A. S. Ito, and H. Jöstlein
State University of New York at Stony Brook
Stony Brook, Long Island, New York 11794

J. A. Appel, B. C. Brown, C. N. Brown, W. R. Innes,
R. D. Kephart, K. Ueno, and T. Yamanouchi
Fermi National Accelerator Laboratory
Batavia, Illinois 60510

S. W. Herb, D. C. Hom, L. M. Lederman,
J. C. Sens,[a] H. D. Snyder, and J. K. Yoh
Columbia University, New York, New York 10027

The mass spectrum of muon pairs in the range 5 to 15 GeV is studied in the inclusive reaction $p + \text{nucleus} \rightarrow \mu^+ + \mu^- + \text{anything}$. The distribution is fitted by a form $d^2\sigma/dm\,dy|_{y=0} = 2.60 \times 10^{-33} \exp(-0.986\ m)\ \text{cm}^2\ \text{GeV}^{-1}\ \text{nucleon}^{-1}$. Comparison with a parton annihilation model yields a sea quark distribution $x\,S(x) = 0.6\ (1 - x)^{10}$. The transverse momentum distribution of the continuum is independent of mass and has a $\langle p_T \rangle$ of 1.19 ± 0.04 GeV. The Υ mean p_T is 1.44 ± 0.11 GeV. The dependence of the continuum production cross section on target atomic weight is presented.

---

[a] Permanent address: Foundation for Fundamental Research on Matter, The Netherlands.

We have recently[1,2] presented data on resonances observed in dimuon production near 9.5 GeV. In this letter, we discuss the dimuon continuum in the mass range 5 to 15 GeV: $p + N \rightarrow \mu^+ + \mu^- +$ anything. Results are based upon 26,000 events observed in the collision of 400 GeV protons with Be, Cu and Pt nuclei.

The experimental apparatus has been described elsewhere.[1,3] Each arm of the double arm spectrometer accepts particles of either sign emitted from 50 to 95 mr horizontally and within ± 12 mr vertically of the incident proton beam. The acceptance as a function of the dilepton mass, p_T, $p_{\parallel}$ and $\cos\theta^*$ (decay angle in dilepton rest system) is determined by these apertures. The functional forms for the distributions of these variables used in the Monte Carlo calculation of the acceptance are suggested by theoretical models. The parameters of these functions are determined from the data. Limited acceptance in $p_{\parallel}$ (or proton-nucleon center of mass rapidity, y) is handled by expressing cross sections at the central value $y = 0$; we are sensitive in the region $-0.3 < y < 0.3$. The residual model dependence arises from limited acceptance in the polar decay angle θ^*. In the Gottfried-Jackson frame, we have assumed the form $1 + \beta\cos^2\theta^*$ and calculated acceptances for $\beta = 0$ and $\beta = 1$. We present the data below using $\beta = 1.0$. For the hypothesis $\beta = 0$, there is a 27% increase in acceptance (decrease in cross section) which is independent of p_T and mass.[4]

There is enough acceptance to permit a study of the decay distribution in the S-channel helicity frame (reference axis along the CM direction in dilepton rest frame). In this frame the distribution is best fit with $\beta \approx 0$.

Table I presents the data, the background (obtained from the like sign muon pairs), the mass acceptance, the differential cross section (with background subtracted) per Pt nucleus, and the cross section per nucleon. Our subtraction of like sign muon pairs corrects for accidentals and muons from the decays of correlated hadrons. We have already[1] demonstrated that resolution tails do not contaminate these data with spill-over from lower mass dimuons.

The reduction of data to "per nucleon" cross sections requires a knowledge of the A-dependence and a study of Fermi motion. We have compared yields in Pt and Be as a function of dilepton mass. Assuming $\sigma \sim A^{\alpha}$, we find that $\alpha = 0.97 \pm 0.05$ averaged over the mass range 5-12 GeV, in agreement with earlier measurements.[5] However, in the following we continue to reduce the data using $\alpha = 1.0$ until a more precise determination is made. The distributions in p_T follow the same fits for the Be target as for the Pt target, indicating that α is not a sensitive function of dilepton p_T for values of p_T less than 3 GeV.[6] We note that the "nucleon" in platinum is 60% n + 40% p.

Fermi motion increases the effective CM energy due to the approximately exponential increase of cross section with energy.[7] We estimated this effect using both a simple Fermi gas model with a maximum momentum of 260 MeV and an experimentally determined Fermi momentum distribution.[8] Using an energy dependence based upon m^2/s scaling, both calculations predict a slope parameter b (Eq. 1) which is 0.03 GeV^{-1} steeper for the per nucleon cross section compared to that of a heavy nucleus. We have divided by A and corrected for Fermi motion to obtain the last column of Table I, Fig. 1, and Table II.

We have fit the resulting data, excluding the 9.0 - 10.8 GeV region, with the form:

$$\left.\frac{d^2\sigma}{dm\,dy}\right|_{y=0} = C\,e^{-bm} \qquad (5.2 < m_{\mu^+\mu^-} < 15) \tag{1}$$

and find:

$$C = 2.60 \pm 0.02 \times 10^{-33}\ \mathrm{cm}^2\ \mathrm{GeV}^{-1}\ \mathrm{nucleon}^{-1}$$

$$b = 0.986 \pm 0.006\ \mathrm{GeV}^{-1}$$

$$\chi^2 = 76 \text{ for } 78 \text{ degrees of freedom.}$$

The errors shown are statistical. The dominant systematic uncertainties in C are ±15% due to $\Delta\alpha$ and $^{+0\%}_{-27\%}$ due to $\Delta\beta$. In addition to these eventually measurable factors, there is an overall normalization uncertainty of ±25%. The systematic error in b is ± 0.02 due to the Fermi motion correction and acceptance uncertainties.

The dominant mechanism for producing the continuum of massive lepton pairs in hadron collisions is expected to be the annihilation of quark-antiquark pairs.[9] At y = 0, the annihilating antiquark from the quark-antiquark sea of one nucleon and the quark from the other nucleon will have $x_1 = x_2 = m/\sqrt{s} \equiv x$. For protons incident on platinum, assuming color and neglecting p_T, the model predicts:

$$\left.\frac{d^2\sigma}{dm\,dy}\right|_{y=0} = \frac{8\pi\alpha^2}{9m^3} \sum_{k=u,d,s} e_k^2\, x^2 \left\{ q_k^{p}(x)\, q_{\bar{k}}^{N}(x) + q_{\bar{k}}^{p}(x)\, q_k^{N}(x) \right\}. \tag{2}$$

The functions $q_k(x)$ $\left(q_{\bar{k}}(x)\right)$ are the fractional momentum distributions for quarks (antiquarks) of flavor k and charge e_k (the superscripts p and N label the beam proton and target nucleon respectively). Using the quark momentum distributions defined by Feynman and Field[10] yields the prediction shown in Fig. 1.

The further assumption that the sea of quark-antiquark pairs is SU(3) symmetric, $q_{\bar{u}}(x) = q_{\bar{d}}(x) = q_s(x) = q_{\bar{s}}(x) \equiv S(x)$, results in a further simplification of Eq. (2):

$$\left.\frac{d^2\sigma}{dm\,dy}\right|_{y=0} = \frac{8\pi\alpha^2}{9m^3}\; x\,S(x)\left\{\nu W_2^{\,p}(x) + \nu W_2^{\,N}(x) - \frac{4}{3}\,x\,S(x)\right\} .$$

$\nu W_2^{\,p}(x)$ and $\nu W_2^{\,N}(x)$ are the inelastic structure functions measured directly in μ-p and e-N inelastic scattering.[11] We find an excellent fit to the data using

$$x\,S(x) = 0.6\,(1-x)^{10} \qquad 0.2 < x < 0.5. \tag{3}$$

Figure 1 shows several curves displaying the sensitivity to $S(x)$.

The statistical precision of the dimuon data require that the effects of scale breaking and quark transverse momenta on Eq. (2) be fully understood before taking Eq. (3) seriously. Recently reported high statistics, high energy lepton scattering data,[11, 12] combined with the dimuon data presented here, will pose a tight constraint on the quark-parton model.

Table II presents the p_T distributions. The large statistical power now clearly determines a shape which can no longer be fit by a simple exponential.[5] All the spectra, excluding the Υ region (9.0 - 10.5 GeV) can be fitted by:

$$E \left. \frac{d^3\sigma}{dp^3} \right|_{y=0} = A\,(m) \quad \left(1 + \frac{p_T^{\,2}}{(2.8)^2}\right)^{-6} \quad .$$

The mean and mean square p_T's are plotted in Fig. 2 together with data[13] at lower mass. There are several conclusions: i) the mean p_T of the dilepton continuum is independent of mass above 5 GeV. ii) the Υ region has a significantly higher $< p_T >$ than the neighboring continuum (if the continuum background is unfolded, the $\Upsilon < p_T > = 1.44 \pm 0.11$ implying a production mechanism which differs from that of the continuum). iii) $m_\perp$ scaling does not hold here, and iv) to the extent that the annihilation model holds, the mean p_T measures directly the mean transverse momentum, k_T, of the annihilating quarks;[14] in fact,

$$< k_T^{\,2} > \; = \; \frac{1}{2} \; < p_T^{\,2} >$$

so that the rms k_T of the quarks is of the order of ~ 1.0 GeV/c.

In summary, we find in the mass range 5-15 GeV a remarkable consistency between the quark-parton model interpretation of the dilepton data and deep inelastic scattering results. In the context of this model we measure the sea quark distribution and the initial state quark transverse momenta. Finally we note that the last row of Table I sets a significant upper limit to the cross section for dilepton production from 15 to 27 GeV.

REFERENCES

[1] S. W. Herb et al., Phys. Rev. Lett. 39, 252 (1977).

[2] W. Innes et al., Phys. Rev. Lett. 39, 1240 (1977).

[3] L. M. Lederman, Proceedings of the European Conference on Particle Physics, Budapest, July 1977. W. R. Innes, Proceedings of the SLAC Topical Conference, Stanford, July 1977.

[4] $B\, d\sigma/dy|_{y=0}$ for Υ depends upon the Υ decay distribution. We now find: for $\beta = 1$, $B\, d\sigma/dy|_{y=0} = 0.27$ pb/nucleon; for $\beta = 0$, $B\, d\sigma/dy|_{y=0} = 0.21$ pb/nucleon.

[5] D. C. Hom et al., Phys. Rev. Lett. 37, 1374 (1976). Note that the high values of $\langle p_T \rangle$ derived in this reference reflect the choice of the fitting function, e^{-bp_T}.

[6] R. L. McCarthy et al. (submitted to Phys. Rev. Lett.) find that for dihadrons, α rises with p_T for $p_T \gtrsim 3$ GeV.

[7] B. G. Pope and L. M. Lederman, Phys. Lett. 66B, 486 (1977).

D. Antreasyan et al., Phys. Rev. Lett. 39, 906 (1977).

[8] P. A. Piroue and J. S. Smith, Phys. Rev. 148, 1315 (1966).

[9] S. D. Drell and T-M. Yan, Phys. Rev. Lett. 25, 316 (1970); Ann. Phys. (N.Y.) 66, 578 (1971).

[10] R. Feynman and R. Field, Phys. Rev. D 15, 2590 (1977).

C. Quigg, private communication.

[11]W. Francis, Division of Particles and Fields Meeting, Argonne National Laboratory (September 1977). T. Kirk, private communication. We have taken the values of $\nu W_2(x, Q^2)$ for $Q^2 = 9$. If we had taken $Q^2 = m^2$ then Eq. (3) would have been $x\ S(x) = 0.5\ (1 - x)^9$.

[12]J. Steinberger, Cargèse Lectures (July 1977).

[13]J. G. Branson et al., Phys. Rev. Lett. 38, 1334 (1977).

[14]See for example C. S. Lam and T-M. Yan, CLNS-365 (1977) and references therein. For an alternative viewpoint see M. Duong-Van et al., SLAC-PUB-1882 (1977). These authors predicted the results of Fig. 2 using C.I.M. However, Kinoshita et al., Phys. Lett. 63B, 355 (1977) did the same via annihilation of high k_T quarks. Still another viewpoint attributes $< k_T >$ to gluon effects treated within QCD as corrections to the basic D-Y process: See Fritzch and Minkowski, Th-2400-CERN (1977); Kajantie and Raitio, HU-TFT-77-21 (Helsinki, 1977).

TABLE I

$M_{\mu^+\mu^-}$	Events		Acceptance	$d^2\sigma/dm\,dy\vert_{y=0}$ (cm^2/GeV)	
GeV/c^2	(+-) + (-+)	(++) + (--)	%	per Pt Nucleus	per Nucleon
5.0 - 5.5	6768	346	0.165	307.0 ± (4.0) x 10^{-35}	159.0 ± (2.1) x 10^{-37}
5.5 - 6.0	5198	104	0.220	183.0 (2.6)	92.8 (1.3)
6.0 - 6.5	3953	23	0.275	113.0 (1.8)	56.4 (0.9)
6.5 - 7.0	2770	8	0.328	66.4 (1.3)	32.8 (0.6)
7.0 - 7.5	2013	2	0.378	41.9 (0.9)	20.4 (0.45)
7.5 - 8.0	1466	0	0.424	27.2 (0.7)	13.0 (0.34)
8.0 - 8.5	986	1	0.467	16.6 (0.5)	7.84 (0.25)
8.5 - 9.0	708	0	0.505	11.0 (0.4)	5.13 (0.19)
Upsilon Region	2106	0	0.570		
10.5 - 11.0	141	0	0.624	1.78 (0.15)	0.78 (0.07)
11.0 - 12.0	125	0	0.657	0.75 (0.07)	0.320 (0.028)
12.0 - 13.0	59	0	0.693	0.33 (0.04)	0.139 (0.018)
13.0 - 14.0	27	0	0.723	0.147 (0.028)	0.059 (0.011)
14.0 - 15.0	10	0	0.753	0.052 (0.016)	0.020 (0.006)
> 15.0	1	0	0.8	< 0.014	< 0.005

TABLE II

Invariant Cross Section ($E\,d^3\sigma/dp^3$) Evaluated at y = 0 vs p_T for Several Mass Bins in Units of 10^{-39} cm^2 GeV^{-2}

p_T (GeV) \ Mass (GeV)	5 - 6	6 - 7	7 - 8	8 - 9	9 - 10.5	> 10.5
0.0 - 0.2	2110±(74)	762 ± (40)	292 ± (23)	127 ± (15)	101 ± (14)	9.0 ± (2.6)
0.2 - 0.4	2090 (49)	703 (24)	264 (13)	97 (8)	107 (8)	8.3 (1.4)
0.4 - 0.6	1756 (42)	662 (20)	240 (11)	95 (6)	86 (6)	6.9 (1.1)
0.6 - 0.8	1584 (42)	537 (17)	196 (9)	80 (5)	72 (5)	5.4 (0.8)
0.8 - 1.0	1174 (37)	439 (17)	166 (8)	59 (4)	59 (4)	6.0 (0.9)
1.0 - 1.2	944 (35)	333 (15)	124 (7)	54 (4)	54 (4)	3.6 (0.6)
1.2 - 1.4	693 (30)	264 (13)	95 (6)	33.2 (3.4)	40 (4)	3.2 (0.6)
1.4 - 1.6	444 (25)	179 (11)	68 (5)	29.0 (3.1)	26.1 (2.8)	2.1 (0.5)
1.6 - 1.8	326 (22)	123 (9)	43 (4)	16.3 (2.3)	20.8 (2.6)	0.89 (0.27)
1.8 - 2.0	228 (19)	81 (8)	26.8 (3.3)	14.2 (2.3)	15.5 (2.2)	1.03 (0.34)
2.0 - 2.2	151 (17)	40 (5)	22.1 (3.2)	8.9 (1.7)	11.6 (1.9)	0.82 (0.31)
2.2 - 2.4	91 (15)	25 (4)	15.7 (2.7)	5.0 (1.2)	7.3 (1.3)	0.32 (0.20)
2.4 - 2.6	66 (13)	25 (4)	6.4 (1.7)	2.5 (0.9)	5.0 (1.3)	0.40 (0.20)
2.6 - 2.8	28 (9)	12.8 (3.2)	5.0 (1.5)	2.1 (0.9)	2.8 (0.9)	0.06 (0.06)
2.8 - 3.0	32 (9)	9.6 (3.0)	4.7 (1.5)	1.1 (0.6)	2.4 (0.9)	0.0 (0.07)
3.0 - 3.2	14 (9)	8.6 (2.6)	3.1 (1.2)	0.6 (0.4)	1.5 (0.6)	0.07 (0.08)
3.2 - 3.4	-3 (7)	7.6 (2.6)	3.3 (1.4)	1.0 (0.6)	2.0 (1.0)	0.09 (0.07)
3.4 - 3.6	34 (16)	1.3 (1.3)	1.4 (0.8)	0.0 (0.4)	0.4 (0.3)	--
3.6 - 3.8	6 (4)	2.2 (1.7)	0.4 (0.4)	0.4 (0.4)	0.9 (0.7)	--
3.8 - 4.0	--	0.8 (0.9)	--	0.3 (0.3)	0.9 (0.6)	--

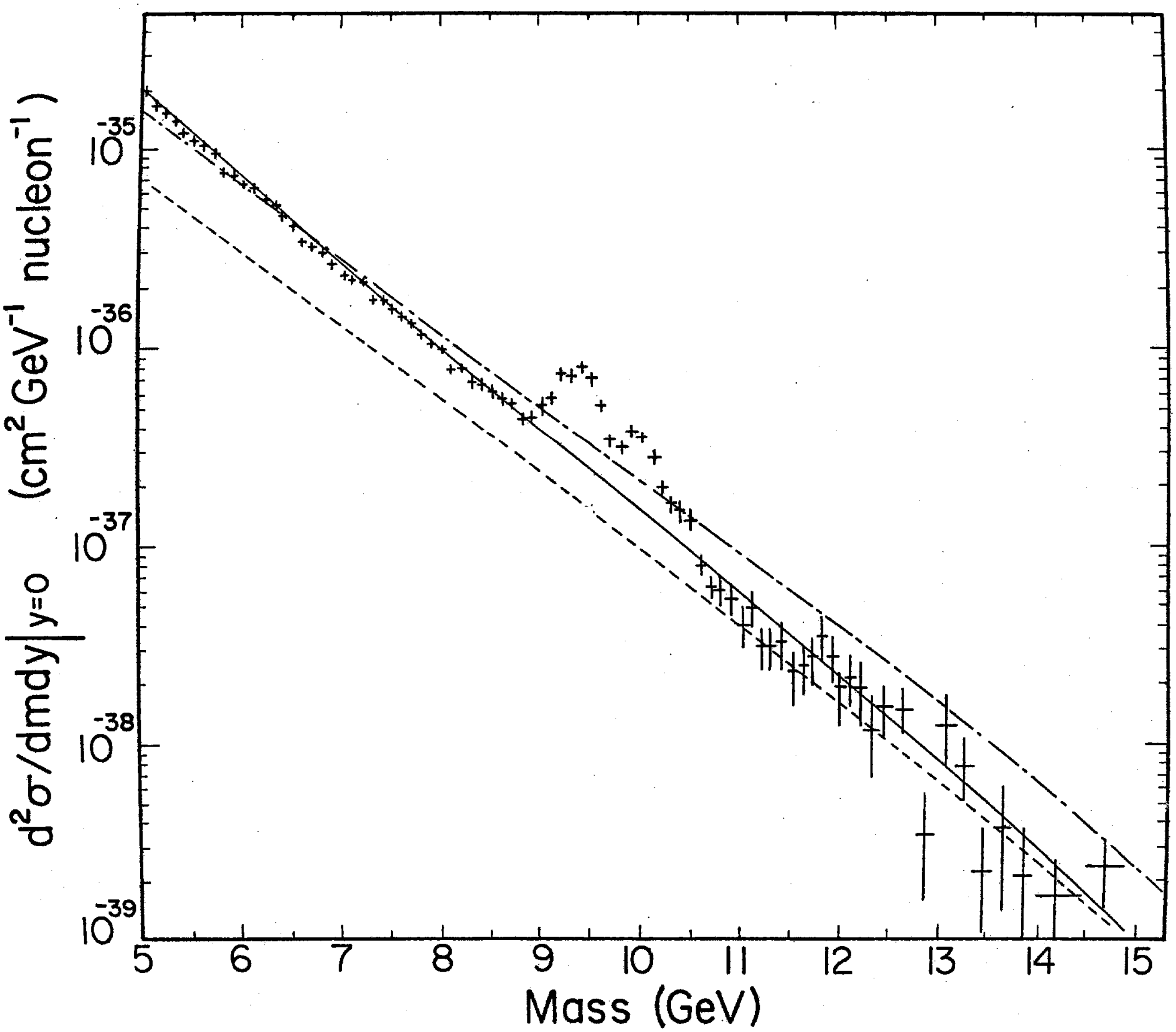

Fig. 1. Cross section for p + "nucleon" → $\mu^+\mu^-$ + X vs. the effective mass of the muon pair. The curves are quark-antiquark annihilation model predictions assuming: solid curve, measured[11] νW_2 and $xS(x) = 0.6(1-x)^{10}$; long-short-dash curve, measured[11] νW_2 and $xS(x) = 0.5(1-x)^8$; short-dash curve, Feynman-Field[10] structure functions.

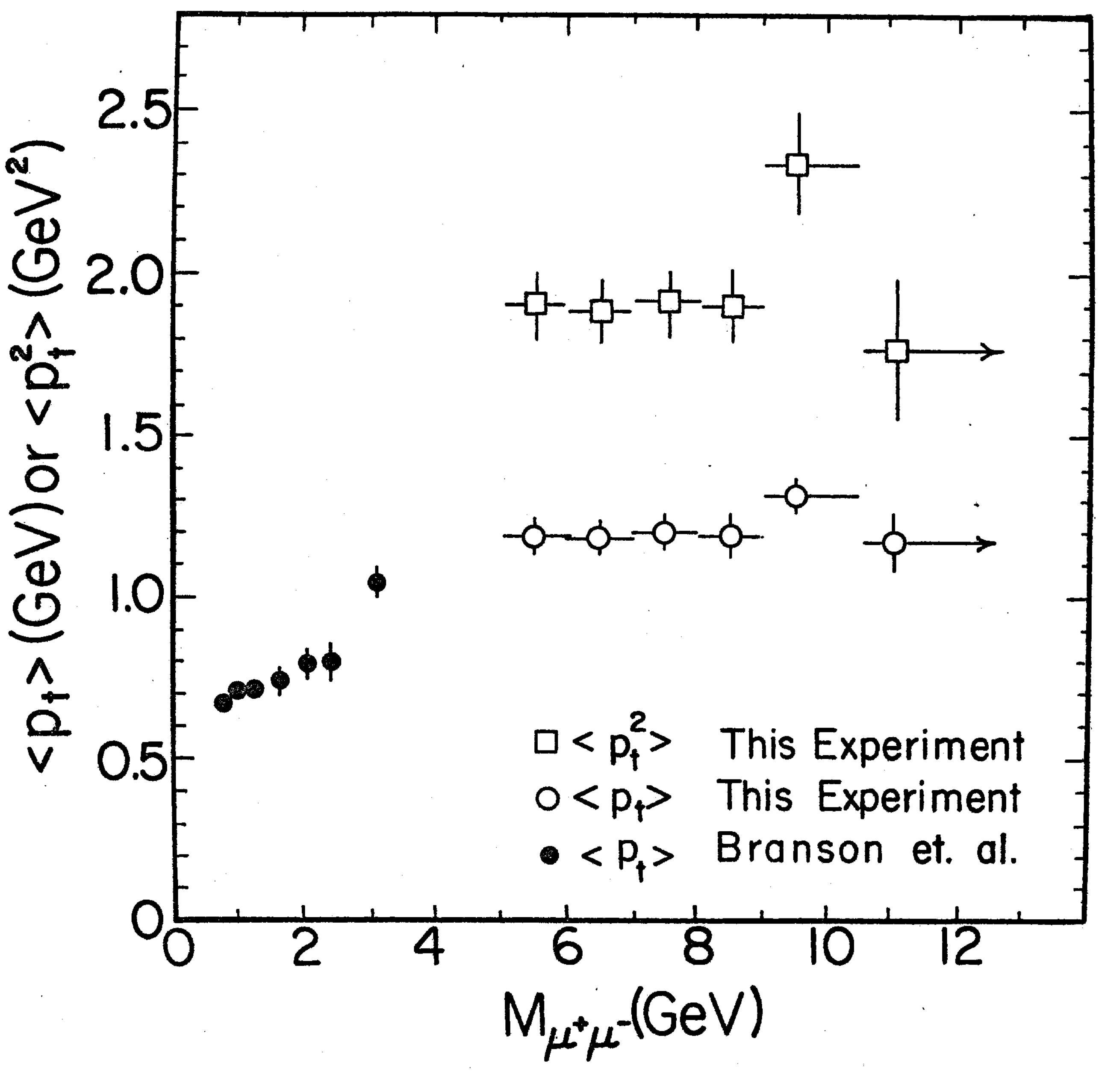

Fig. 2. Mean p_T and mean square p_T of the muon pairs vs. effective mass. The data of Branson et al. are from Ref. 13.